MODELLING AND CONTROL OF AN ONBOARD FUEL PROCESSOR FOR INDIRECT METHANOL FUEL CELL VEHICLES

Alessandro Miotti, **Riccardo Scattolini**

Dipartimento di Elettronica e Informazione,
Politecnico di Milano, 20133 Milano, Italy
{miotti,scattolini}@elet.polimi.it

Abstract
In this paper, the dynamic model of a fuel processor for hydrogen production from steam reformation is first introduced. The fuel processor is built according to an integrated burner and reformer bi-catalyst plate configuration. The model is then coupled with the one of a PEM fuel cell, and the overall simulator is used to analyze different control configurations. It is shown that the limited dynamic performances of the fuel processor do no represent a critical obstacle for future on-board applications provided that a proper architecture of the system and a well designed control structure are used.

1. INTRODUCTION

The increasing interest of the automotive industry in hydrogen fueled PEM fuel cells is motivated by their significant advantages in terms of efficiency and reduced pollutants emissions. However, the wide diffusion of fuel cell vehicles is still seriously hampered by the existing limitations in the distribution and storage of hydrogen. A possible solution consists in the use of on-board fuel processors for hydrogen production from steam reformation of methanol or other hydrocarbons. Since this is an endothermic process, the overall system requires also a catalytic burner to supply the required thermal energy, see e.g. (Geyer, 1996; Ohl, 1995; Dams *et al.*, 2000; Driel *et al.*, 1998; Cunha and Azevedo, 2000) where different thecnological solutions are presented and discussed. Among them, the candidates for a practical on-board implementation are those guaranteeing sufficient dynamical performances, in terms of transient responses, with limited weight and dimensions. In this respect, the thermally integrated burner and reformer bi-catalyst plate configuration analyzed in (Dams *et al.*, 2000; Driel *et al.*, 1998; Cunha and Azevedo, 2000) appears to provide the necessary speed of heat transfer from the burner to the reformer. As such, it has been considered in this study, aimed at analysing, through a detailed simulation model, the dynamic performances and the control configurations of a steam reforming unit coupled with a fuel cell. In the following sections, a dynamic model of the fuel processor is first derived starting from the results discussed in (Sundaresan and al., 2000; Sundaresan and al., 2003). The characteristics of this model, as well as their dependence on some parameters such as the heat exchange coefficients, are then studied through simulations and by analyzing the corresponding linearized system. Finally, the fuel processor model is coupled with the one of a fuel cell, basically derived from (Pukrushpan *et al.*, 2002) and not reported here for space limitations, and different control strategies are examined. Notably, the focus here is not on the tuning of the adopted regulators, which are implemented as standard PI controllers, but rather on the control schemes. To this regard, it is shown that the insertion of a simple hydrogen storage system between the fuel processor and the fuel cell can significantly reduce the problems due to the limited dynamic behaviour of the hydrogen production unit.

2. FUEL PROCESSOR MODEL

The overall fuel processor consists of a steam reformer, a catalytic burner, a mixer, a preheater, a *CO* clean-up and an air supply system. The fuel (methanol) stored in a tank is sent to the burner and to the reformer. The burner is also supplied with air through a compressor to feed the combustion providing the reformer with the required heat. The reformer is feeded with a heated mixture of steam and methanol, which react to produce hydrogen, and with residual H_2 from the fuel cell stack anode. The outcomes of the reaction are H_2, CO_2 and a small quantity of *CO*, which are subsequently removed to produce high purity H_2 as required by the fuel cell.

In this study, only the reformer and the burner have been modelled. They have been assumed to be integrated according to a bi-catalytic plate configuration, where one side of each plate is coated with the reformer catalyst and the other side with the burner catalyst. Both the reactors have been modeled as PFR (Plug Flow Reactors), represented by a series of CSTR (Continuous Stirred Tank Reactors) of equal size, thus implicitely assuming that all the quantities are changing along a discretized axial coordinate, while they have been taken as constant inside a single CSTR.

The physical model has been derived under the following main assumptions: (i) every CSTR is described by a lumped parameters model, (ii) the pressure P inside the reactors has been set equal to the atmospheric pressure, (iii) the gas mixture is an ideal gas, (iv) heat exchanges with the external environment have been ignored, (v) homogeneous reactions have been considered inside each reactor. This last assumption is introduced to limit the order of the overall model, and is justified by the results presented in (Sundaresan and al., 2000; Ito *et al.*, 1990).

2.1 Burner

For each CSTR describing the burner, the dynamic model has been derived as follows (see also (Sundaresan and al., 2003; Sunderasan and al., 2000)). The combustion reaction rate of methanol and air at atmospheric pressure has been computed on the basis of the one-step Arrhenius law for complete oxidation on platinum, with zero-order reaction for oxygen and first order reaction for methanol, see (Ito *et al.*, 1990). The methanol oxidation equation is

$$CH_3OH + 1.5O_2 = CO_2 + 2H_2O$$

and its homogeneous reaction rate is

$$r_{CH_3OH} = kC_{CH_3OH}V \tag{1}$$

where C_{CH_3OH} is the methanol concentration in the gas, V is the volume of the CSTR and k is the reaction rate constant given by

$$k = e^{\left(\frac{6.1*10^3}{RT_b}+3.2\right)} \tag{2}$$

R is the universal gas constant and T_b is the (average) temperature inside the CSTR. The reaction rates of all other species (O_2, CO_2, H_2O) can be obtained from the soichiomeric coefficients.

For each CSTR, letting n_i be the quantity (mol) of the $i-th$ specie, $F_{i(IN)}$ and F_i its input and output flowrates and r_i the reaction rate, the mass balance equation for each specie is

$$\frac{dn_i}{dt} = F_{i(IN)} - r_i - F_i \tag{3}$$

The total number of moles $n_T = PV/RT_b$ is obtained from the ideal gas law. Moreover, letting F_T be the total output flowrate, one has

$$F_i = \frac{n_i F_T}{n_T} \tag{4}$$

and

$$F_T = \sum F_{i(IN)} - \sum r_i + \frac{PV}{RT_b^2}\frac{dT_b}{dt} \tag{5}$$

The energy balance equation is

$$\begin{aligned}\frac{dE}{dt} &= \sum F_{i(IN)}h_{i(IN)} + \\ &- \sum \left(F_i + \frac{dn_i}{dt}\right)h_i - U_{bw}A(T_b - T_w)\end{aligned} \tag{6}$$

where $E = m_b c_{p_b} T_b$ is the total energy inside the CSTR, m_b is the burner mass, c_{p_b} is the specific heat of the burner, $h_{i(IN)}$ is the enthalpy of the input flowrate of the $i-th$ specie, h_i is the corresponding enthalpy inside the reactor, T_w is the temperature of the wall, A is the reaction surface area and U_{bw} is the heat transfer coefficient between the burner and the wall. Furthermore, $h_i = c_{pi}T_b$ where the constant pressure specific heat c_{pi} is computed as

$$c_{pi} = a_i + b_i T + c_i T^2 + d_i T^3 \tag{7}$$

and a_i, b_i, c_i, d_i are experimental coefficients, see (Cengel, 1997).

2.2 Reformer

Also the reformer has been modelled as a series of CSTR, each one described by a couple of mass and energy balance equations with the same structure of (3)-(7). The computation of the kinetic constants as well as of the reaction rates has been based on experimental results, see (Amphlett and al., 1994), obtained for an homogeneous reaction with a catalyst made

by $CuO/ZnO/Al_2O_3$. The reaction rates of the five components of the reaction are

$$\begin{cases} r_{H_2} &= 3k_1C_{CH_3OH} + 2k_2 \\ r_{CH_3OH} &= -k_1C_{CH_3OH} - k_2 \\ r_{CO_2} &= k_1C_{CH_3OH} \\ r_{H_2O} &= -k_1C_{CH_3OH} \\ r_{CO} &= k_2 \end{cases} \tag{8}$$

where k_1 and k_2 are given by

$$\begin{aligned} k_1 &= \frac{[A_1 + B_1 \ln(\frac{s}{M})]\exp(\frac{E_1}{RT})}{P^{C_1}} \\ k_2 &= \frac{A_2 \exp(\frac{-E_2}{RT})}{P^{C_2}} \end{aligned} \tag{9}$$

E_1 e E_2 are the Arrhenius activation energies, s/M is the vapour/methanol ratio and A_i, B_i, C_i are experimental coefficients.
For each CSTR the energy balance equation is:

$$\begin{aligned} \frac{dE_r}{dt} &= \sum F_{i(IN)}h_{i(IN)} + \\ &- \sum \left(F_i + \frac{dn_i}{dt}\right) h_i - U_{rw}A\,(T_w - T_r) \end{aligned} \tag{10}$$

where $E_r = mc_pT_r$ is the total energy inside the CSTR, m_r is the mass, c_{p_r} is the specific heat, T_r is the temperature and U_{rw} is the heat transfer coefficient between the reformer and the wall

2.3 Wall

The wall provides the thermal coupling between the burner and the reformer, and is simply described by the following energy balance equation

$$\begin{aligned} (m_wc_{p_w})\frac{dT_w}{dt} &= U_{bw}A(T_b - T_w) + \\ &- U_{rw}A(T_w - T_r) \end{aligned} \tag{11}$$

where m_w and c_{p_w} are the mass and the constant pressure specific heat respectively.

3. OPEN-LOOP ANALYSIS

The dynamic model described in the previous section has been implemented in the Matlab/Simulink environment and a number of open-loop simulations have been performed to analyse the transients of the temperatures T_b, T_w, T_r and of the produced hydrogen due to step changes of the incoming methanol flowrate.

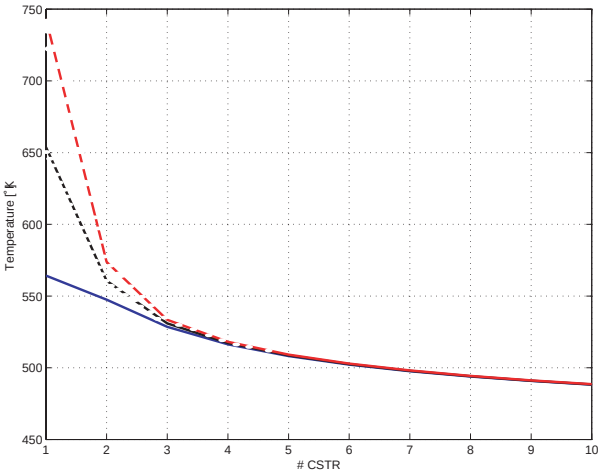

Figure 1. Temperatures profile along the reactors at steady state. T_b(dashed),T_w(dotted),T_r(solid).

3.1 Simulation data

Table 1. Simulation Data

Parameter	Value
Reactor volume	$4dm^3$
Reactor length	$0.065m$
Open frontal area fraction	0.64
Reformer weight	$35kg$
Burner weight	$6kg$
Endothermic energy (reformer)	$48kJ/mole$
Exothermic energy (burner)	$726kJ/mole$
Fuel Cell Power	$45kW$
Fuel Cell Anode volume	$0.005m^3$

The choice of the number of CSTR used to model both reactors is dictated by a compromise between computational times and the desired accuracy. According with the literature, ten CSTR have been revealed to be a good solution. The main simulation data are reported in Table 1. Another important parameter is the heat transfer coefficient between the burner and the reformer, which has been chosen in nominal conditions as $200W/(m^2K)$.Yet some simulations with different values of this coefficient have been done.

3.2 Thermal Integration

The computed steady state temperatures profile corresponding to a methanol input flowrate of 0.3 mol/s for the reformer and 0.033 mol/s for the burner is shown in Fig.1. It is apparent that the adopted bi-catalyst plate configuration guarantees an excellent thermal coupling between the two reactors, which maintain similar temperatures. In turn, this corresponds to a limited production of NO_x and to faster thermal transients.
A second set of simulation experiments has been aimed at analyzing the influence of the thermal cou-

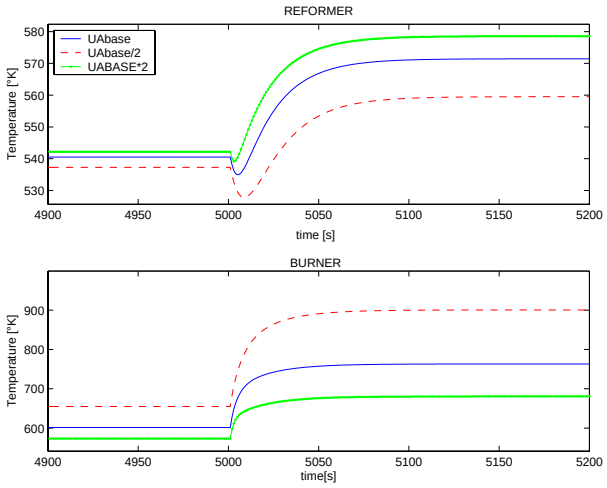

Figure 2. Temperature in the first CSTR of the burner and of the reformer due to a step change of the incoming methanol flowrate.

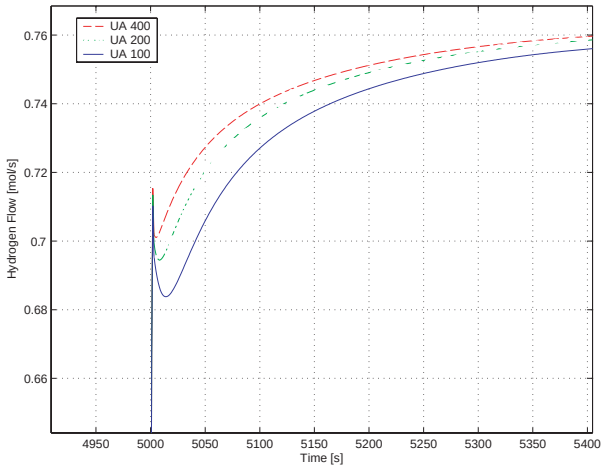

Figure 3. Outlet H_2 flowrate due to a step change of the incoming methanol flowrate.

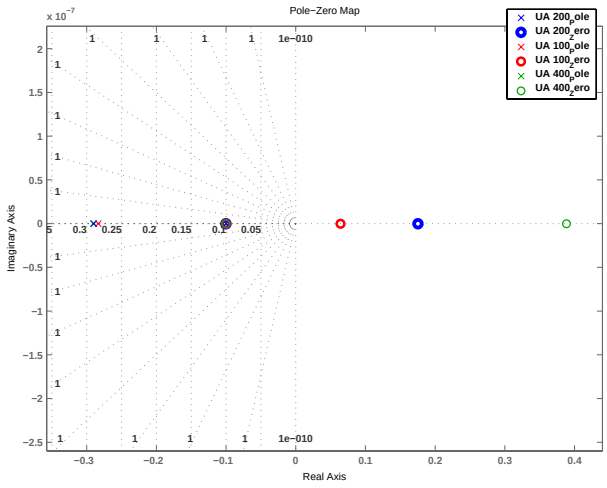

Figure 4. Dominant pole and zero for different values of UA.

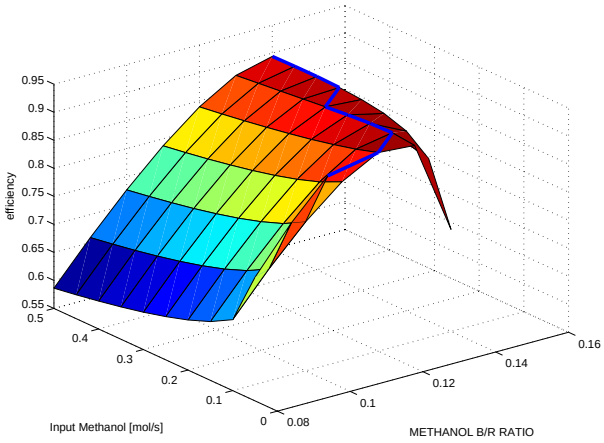

Figure 5. Efficiency η as function of the methanol flowrate to the reformer and of the burner/reformer methanol flowrate ratio.

pling, which can be described by the parameter $UA = U_{bw}A * U_{rw}A$. Starting from steady state conditions, in Fig.2 it is shown the effect of a step change of amplitude 0.2mol/s of the methanol input flowrate to the burner and to the reformer. These results show that a better thermal coupling leads to a smaller T_b and a higher T_r, that is to a minor production of NO_x and to a larger H_2 production, see Fig.3. However, also the production of CO is increased, so that the role of the CO clean-up becomes fundamental. Finally, it is apparent from Fig.2 that the "inverse response", or "nonminimum-phase", effect in the response of T_r is reduced. This result is confirmed by the analysis of the pole/zero configuration of the transfer function of the linearized system between methanol input flowrate and reformer output temperature, see Fig.4 where the dominant pole and the dominant zero are plotted for different values of UA. In conclusion, a better thermal coupling makes easier the design of the control scheme regulating the H_2 output flowrate and leads to fuel savings, because a smaller quantity of methanol is required to produce the same quantity of H_2, see Fig.3.

4. FUEL PROCESSOR CONTROL DESIGN

The goal of the fuel processor control scheme is to provide at any time instant the required hydrogen to the fuel cell stack with the minimum methanol consumption. To this end, four input variables are a priori available, namely, methanol and air flowrates to the burner and methanol and vapour flowrates to the reformer. As a matter of fact, simple stoichiometric computations are sufficient to conclude that the ratio between air and methanol to the burner must be set to 1.5, while the ratio between vapour and methanol to the reformer should be equal to one. In practice, it has been shown, see (Mohilla and Ferencz, 1982), that it is better to set this second ratio to a slightly larger value, for example 1.3, so as to increase the reaction rate inside the reformer. Moreover, it is also advisable to derive the methanol flowrate to the burner

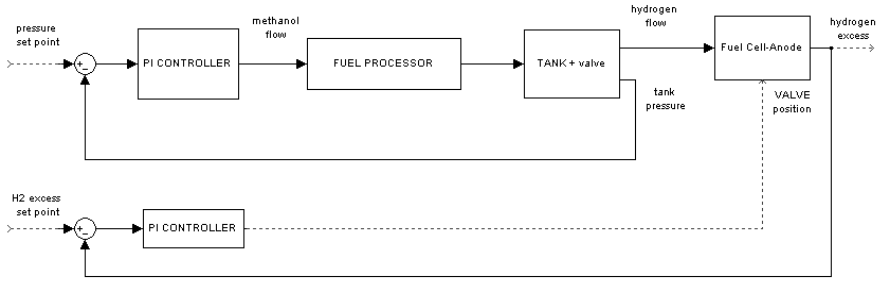

Figure 8. Control scheme with a storage tank between the fuel processor and the fuel cell.

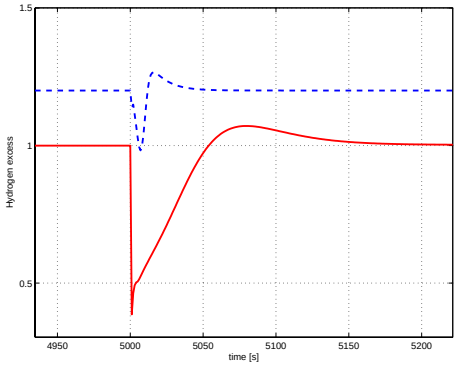

Figure 6. Transient of H_2 excess due to a step load variation from 50A to 250A. a)regulation of H_2 excess(dashed); b)regulation of H_2 flowrate (solid).

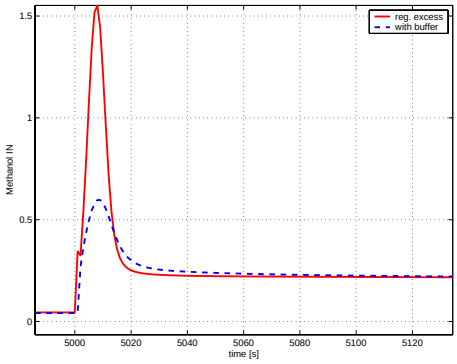

Figure 7. Intake methanol flowrate to the reformer for a step load variation from 50 to 250 A. a)regulation of H_2 excess(solid); b)with tank (dashed).

from the one to the reformer in order to maximize the overall efficiency η defined by (see (Ramaswamy *et al.*, 2000))

$$\eta = \frac{H_{2out} LHV_{H_2}}{F_{Met-IN} LHV_{Met}} \tag{12}$$

where LHV_x is the lower heating power of x and F_{Met-IN} is the total (to the burner and to the reformer) input flowrate of methanol. Fig.5 shows the efficiency η as function of the methanol flowrate to the reformer and of the burner/reformer methanol flowrate ratio. In view of these considerations, also the methanol flowrate to the burner must be computed (through the

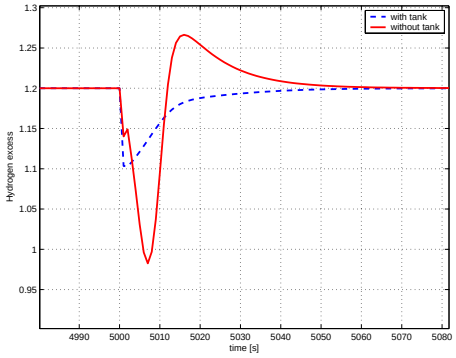

Figure 9. Hydrogen flowrate variation due to a step load: with and without a storage tank.

static map shown in Fig.5) from the methanol flowrate to the reformer $F_{Met-rIN}$, which turns out to be the only independent variable.

The simplest feedback control scheme computes the control variable $F_{Met-rIN}$ on the basis of the error $e_{H_2} = H_2^o - H_2$, where H_2 is the flowrate from the fuel processor to the fuel cell, while H_2^o is a reference signal obtained through a static map relating the current load of the fuel cell and the hydrogen reference value. However, this control scheme turns out to be unsatisfactory due to the limited dynamic performances of the fuel processor. In fact, sudden current load variations cause an immediate increase of the hydrogen reference value, which cannot be provided by the fuel processor with the required speed due to its limited dynamic performances. This causes the reduction of hydrogen in the cell anode, with dramatic effects on the overall system behaviour.

Alternatively, it is possible to control the excess of hydrogen inside the cell instead of the hydrogen itself, that is to use a value of H_2^o higher than the nominal one. This guarantees that during the transients caused by load variations, the hydrogen inside the cell always exceeds a safety threshold. In Fig.6 it is shown the transient of the hydrogen inside the anode due to a step load variation from 50A to 250A with the the excess of hydrogen set to 1 and to 1.2 respectively. In both cases, the regulators are PI's properly tuned starting from the linearized process model. From Fig.6 it is apparent that when the set-point of the hydrogen excess is equal to one, the hydrogen inside the cell

temporarily reaches very low values, with the potential damage of the cell itself. On the contrary, when the reference value is set to 1.2, safety conditions are guaranteed. As a drawback, the proposed control strategy causes an increase of the fuel consumption. For example, a H_2 excess of 30% corresponds to an increased consumption of about 10% of the methanol required to produce the same power. However, notice that the hydrogen not used in the fuel cell can be burned inside the fuel processor, so leading to fuel saving. Finally, as shown in Fig.7, in order to achieve satisfactory dynamic performances, the proposed control strategy produces a very solicited control variable, in particular in the first instants following the load step change.

To compensate for this effect, and to guarantee a much safer and smoother control action, it is here suggested to include in the system a buffer, that is a hydrogen storage tank, between the fuel processor and the fuel cell stack system. In this case, the adopted control scheme is shown in Fig.8. Note that the regulation of the hydrogen inside the cell anode does not directly depend now on the dynamics of the fuel processor, but only on the valve regulating the hydrogen flow from the tank, while the fuel processor is controlled to keep constant the pressure inside the tank. This solution has a twofold advantage. First, it calls for a reduction of the fuel consumption, see again Fig.7. Second, it leads to reduced oscillations of the hydrogen level inside the anode, with minor stress and much safer operating conditions. These conclusions are confirmed by the results reported in Figs.7 and 9 and obtained in simulation by enlarging the overall simulator with a couple of mass and energy balance equations modelling the hydrogen storage tank. Remarkably, in view of the better transients responses shown in Fig.9, it is also possible to reduce the reference value of the hydrogen excess, with a considerable improvement of the overall system efficiency.

5. CONCLUSIONS

In this paper, the modelling and control of a fuel processor system have been considered. The fuel processor dynamic model has been coupled with the one of a fuel cell to develop a preliminary study of the mutual influence of the two elements. A number of control structures have been analyzed, and it has been shown that the use of an auxiliary small storage tank between the fuel processor and the fuel cell, coupled with a proper control scheme, can significantly reduce the problems due to the different dynamics of the processor and of the cell.

6. ACKNOWLEDGMENTS

The authors acknowledge the help provided by Dr.J.T. Pukrushpan, Automotive Research center at University of Michigan, in the development of the fuel cell model.

REFERENCES

Amphlett, J.C. and al. (1994). Hydrogen production by steam reforming of methanol for polymer electrolyte fuel cell. *Journal of Hydrogen Energy* **19**(2), 131–137.

Cengel, A.Yunus (1997). *Introduction to Thermodyanamic and Heat Transfer*. McGraw Hill.

Cunha, J. and J.L.T Azevedo (2000). Modeling the integration of a compact plate steam reformer in a fuel cell system. *Power Sources 86* **34**, 515–522.

Dams, R.A.J., P.R. Hayter and S.C. Moore (2000). The development and evaluation of compact, fast response integrated methanol reforming fuel processor systems for pemfc electric vehicles. *SAE paper No.2000-01-0010*.

Driel, Van, Marinus, Meijer and Marianne (1998). A novel compact steam reformer for fuel cells, with heat generation by catalytic combustion augmented by induction heating. *1998 Fuel Cell seminar, Palm Springs, CA*.

Geyer, H.K. (1996). Dynamic response of steam-reformed, methanol-fueled, polymer electrolyte fuel cell systems. *Proceedings of the 31st IECEC* **2**, 1101.

Ito, K., B.C. Choi and O. Fujita (1990). The start-up characteristic of a catalytic combustor using a methanol mixture. *JSME Int. J., Ser.II 33 (4)* **2**(33), 778–784.

Mohilla, R. and B. Ferencz (1982). *Chemical process dynamics*. Elsevier Scientific Publishing Co.

Ohl, G.L. (1995). Dynamic analysis of a methanol to hydrogen steam reformer for transportation application. *Ph.D Dissertation. University of Michigan*.

Pukrushpan, J.T., A.g. Stefanopulou and H. Peng (2002). Modeling and control for pem fuel cell stack system. *Proceeding of American Control Conference* pp. 3117–3122. Anchorage,AK.

Ramaswamy, S., M. Sundaresan and R.M. Moore (2000). Impact of reformer/burner thermal integration on the efficiency and dynamic of an on-board fuel processor in an indirect methanol fuel cell vehicle. *Int. Mechanical Eng. Congress and exposition*.

Sundaresan, M. and al. (2000). Steam reformer/burner integration and analysis for an indirect methanol methanol fuel cell vehicle. *AIAA-2000-3047* , 1367–1371.

Sundaresan, M. and al. (2003). Catalytic burner for an indirect methanol fuel cell vehicle fuel processor. *Journal of Power Sources* (113), 19–36.

Sunderasan, M. and al. (2000). Modeling a catalytic combustor for a steam reformer in a methanol fuel cell vehicle. *Int. Mechanical Eng. Congress and Exposition*.